Comprehensive Identification of Genomic and Environmental Determinants of Phenotypic Plasticity in Maize

Laura E. Tibbs-Cortes[1,2,3], Tingting Guo[4,5], Carson M. Andorf[3,6], Xianran Li[2,*], Jianming Yu[1,*]

Supplemental Materials

Table of Contents:

- Fig. S12: BRIDGEcereal visualization of major haplotypes for DTA slope candidate genes and associated phenotype estimates among the NAM founders.
- Fig. S13: BRIDGEcereal visualization of major haplotypes for *cct1*, the candidate gene identified for both DTA slope and intercept, and associated phenotype estimates among the NAM founders.
- Fig. S14: Study environments map.
- Fig. S15: Relationship between heritability and degree of plasticity.
- Fig. S16: Prediction accuracy for Anthesis-Silking Interval (ASI) with and without moisture variables.

Supplemental Tables

- Table S1: List of traits.
- Table S2: CERIS-chosen environmental indices.
- Table S3: Significant markers. (Note: Table S3 is attached as "Supplemental_Table_S3.csv")
- Table S4: Candidate genes. (Note: Table S4 is attached as "Supplemental_Table_S4.csv")
- Table S5: Enriched GO terms.
- Table S6: Within-environment heritability.

Supplemental Code Files

- Supplemental Code File 1: Code used in this manuscript. (Note: attached as Supplemental_Code_File_1.R)

Supplemental Methods

Assessment of Impacts of Environment Number on Accuracy of CERIS

Recent work systematically evaluated the number of environments needed to accurately estimate and predict slope and intercept with empirical data from two crops (Guo et al. 2024). These results showed that it is not only the number of environments observed but also the range of the environmental mean that they cover that contributes to the accuracy of reaction norm parameter estimates (Guo et al. 2024). From sampling subsets of a total of 9 environments, a plateau in accuracy was consistently observed in both intercept and slope estimates in both crops when the subset included at least 4 environments and/or covered an environmental mean range at least 25-50% of the minimum environmental mean observed (Guo et al. 2024). As few as two environments could provide good estimates, as long as they covered a wide environmental gradient.

To check for impacts of number of observed environments on prediction accuracies, we examined the correlation between these and found a significant positive correlation (Fig. S7A: $r = 0.47$, $P < 0.001$). However, those traits regarded as important and requiring less additional work beyond the field observations were measured in more environments (e.g., n=11 environments for flowering traits DTA and DTS, considered less complex to predict) than were yield traits that require harvesting and processing for measurements (e.g., n=5 environments for yield traits T20KW and KN, considered more complex to predict) (Table S1) (Onogi 2022; Li et al. 2021). To differentiate the relative importance of trait type and environment number to the overall trend, we checked the correlation within trait type, and found that correlations decreased notably (Fig. S7B, $r = 0.26$-0.30, $P<0.001$), indicating that much of the overall trend came from the connection of trait type (and prediction complexity) with observation number.

The range of measured environment number was 5-11 for all traits and an environmental mean range of at least 25% of the minimum environmental mean was observed for all but 4 traits (ERN, CD, LL, and T20KW), indicating that our data likely reached the plateau found by (Guo et al. 2024) based on the number of environments and therefore should provide accurate estimates of slope and intercept,

though of course there may be room for further improvement, particularly for the traits for which a lower environmental range was covered.

Construction of Candidate Gene List

The full candidate gene list (Table S4) was constructed by building on previous work in the NAM panel that defined candidate genes as those within a 20kb window centered on each significant marker from GWAS (Kusmec et al. 2017). Each significant marker has segregating (bi-allelic) variants in the NAM and was found to be associated with trait variation using GWAS. In general, choosing an appropriate window for candidate gene identification is always a challenging topic and a subject of future research. Therefore, we checked 13 different window sizes (4kb, 10kb, 20kb, 30kb, 40kb, 60kb, 80kb, 100kb, 150kb, 200kb, and 250kb) to confirm consistency of general patterns (Fig. S10). The chosen 20kb window corresponds to an average LD (r^2) of 0.16 in our data, which is within the typical r^2 range of 0.1 – 0.2 for delineating candidate regions (Vos et al. 2017). To enable readers to investigate other windows, we also made all significant SNPs available in Table S3 as well as at MaizeGDB.

The candidate gene list was based on the current B73 genome assembly (Zm-B73-REFERENCE-NAM-5.0) for several reasons. First, in the maize NAM population, approximately 50% of the genetic material of a given RIL originates from B73 and the other 50% from another NAM parent. In the population as a whole, therefore, 50% of the genetic material originates from B73, while only ~1.9% originates from each of the other parents (Yu et al. 2008), providing substantially less confidence in any inferences about non-core candidate genes sourced from other (non-B73) NAM parents vs. those found in B73. In addition, the recent re-sequencing of the NAM founders, which generated the high-density SNP and SV marker data utilized here, mapped all markers to the B73 genome (Hufford et al. 2021). It was cleaner to keep the annotations consistent with the genomic coordinates used to identify these SNPs and SVs. Finally, because by definition core genes are present in all annotations, our method did not exclude any core genes. Therefore, we focused on B73 genes in our investigation. In doing so, we also follow

established precedent for GWAS in this population (Hufford et al. 2021) and for other cases with pan-genomes available (Della Coletta et al. 2021).

Based on the >20 million SNP and SV markers used for GWAS, 94% of the candidate genes identified had at least one SNP or SV marker within the gene itself, increasing to >99% when the search was broadened to include 5kb upstream. Among the remaining genes, manual examination revealed non-marker polymorphisms; for example, Zm00001eb036690 had no markers within it, but BRIDGEcereal identified large indels within this gene among the NAM founders. Because of the presence of non-marker polymorphisms as well as our goal to provide a community resource with all significant results available for ongoing investigation, we chose to retain the remaining <1% of genes from our candidate gene list.

BRIDGEcereal Haplotype Visualization

BRIDGEcereal (https://bridgecereal.scinet.usda.gov/) (Zhang et al. 2023) was used to manually identify indel-based haplotypes among the NAM parents for a subset of the candidate genes ("selected" candidate genes) in the example trait DTA (Fig. S11, Fig. S12, Fig. S13). For each gene, the 26 parents were grouped into two or three "genotype groups," representing different BRIDGEcereal-detected haplotypes based on large indels, which were then named after a representative parent in that group. The phenotype estimates for each NAM parent within a given genotype group were also plotted (Fig. S11, Fig. S12, Fig. S13).

Supplemental Methods Sources

Della Coletta R, Qiu Y, Ou S, Hufford MB, Hirsch CN. 2021. How the pan-genome is changing crop genomics and improvement. *Genome Biol* **22**: 3.

Guo T, Wei J, Li X, Yu J. 2024. Environmental context of phenotypic plasticity in flowering time in sorghum and rice. *J Exp Bot* **75**: 1004–1015.

Hufford MB, Seetharam AS, Woodhouse MR, Chougule KM, Ou S, Liu J, Ricci WA, Guo T,

Olson A, Qiu Y, et al. 2021. De novo assembly, annotation, and comparative analysis of 26 diverse maize genomes. *Science* **373**: 655–662.

Kusmec A, Srinivasan S, Nettleton D, Schnable PS. 2017. Distinct genetic architectures for phenotype means and plasticities in Zea mays. *Nat Plants* **3**: 715–723.

Li X, Guo T, Wang J, Bekele WA, Sukumaran S, Vanous AE, McNellie JP, Tibbs-Cortes L, Lopes MS, Lamkey KR, et al. 2021. An integrated framework reinstating the environmental dimension for GWAS and genomic selection in crops. *Mol Plant* **14**: 874–887.

Onogi A. 2022. Integration of Crop Growth Models and Genomic PredictionGenomic predictions (GP). In *Genomic Prediction of Complex Traits: Methods and Protocols* (eds. N. Ahmadi and J. Bartholomé), pp. 359–396, Springer US, New York, NY.

Vos PG, Paulo MJ, Voorrips RE, Visser RGF, van Eck HJ, van Eeuwijk FA. 2017. Evaluation of LD decay and various LD-decay estimators in simulated and SNP-array data of tetraploid potato. *TAG Theor Appl Genet Theor Angew Genet* **130**: 123–135.

Yu J, Holland JB, Mcmullen MD, Buckler ES. 2008. Genetic Design and Statistical Power of Nested Association Mapping in Maize. *Genetics* **178**: 539–551.

Zhang B, Huang H, Tibbs-Cortes LE, Vanous A, Zhang Z, Sanguinet K, Garland-Campbell KA, Yu J, Li X. 2023. Streamline unsupervised machine learning to survey and graph indel-based haplotypes from pan-genomes. *Mol Plant* **16**: 975–978.

Supplemental Figures

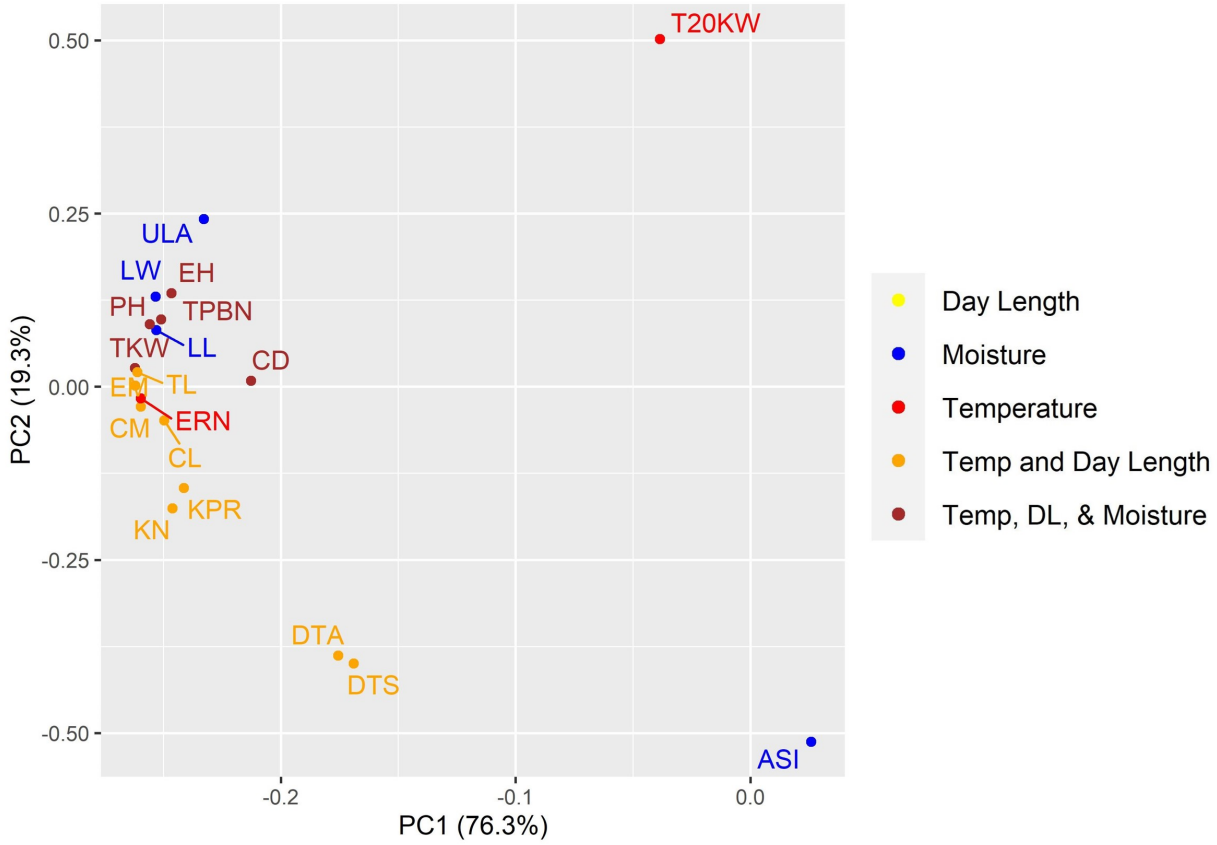

Fig. S1: Principal Components Analysis (PCA) of environmental means reflect environmental indices identified by CERIS. Principal Components (PCs) were calculated based on the scaled and centered environmental mean for each trait; percent of variance explained by each PC is shown on axes. Traits are colored by the environmental variable(s) chosen for them by CERIS. Abbreviations: temperature (temp) and day length (DL).

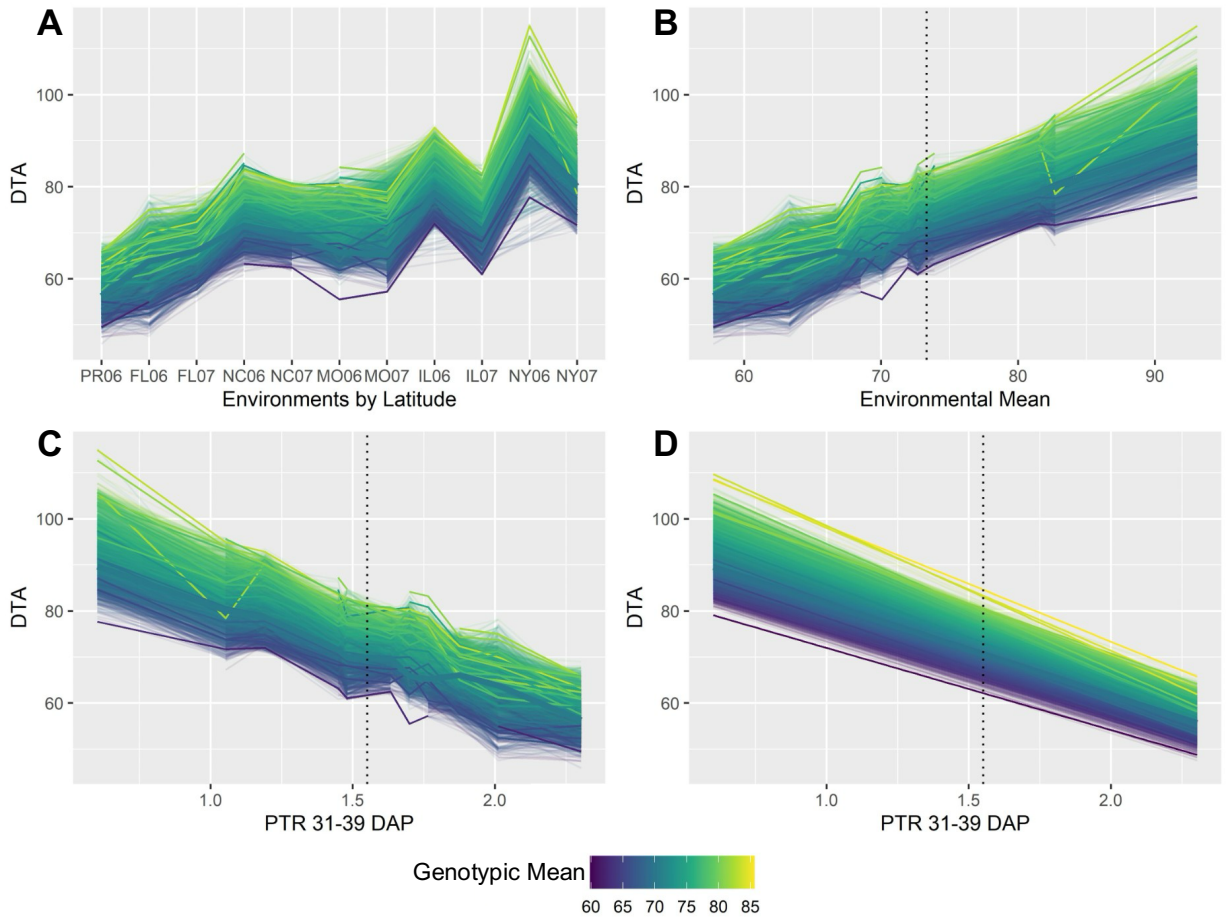

147

148 Fig. S2: Pattern detection for phenotypic plasticity of days to anthesis (DTA) in the maize NAM
149 population. (A) DTA across environments ordered by latitude. Environments are named as the
150 two-letter state abbreviation with the last two digits of the year (e.g., MO06 is Missouri 2006).
151 (B) DTA across environmental mean values. (C) DTA across values of the CERIS-selected
152 environmental index (PTR 31-39 DAP). (D) Linear reaction norm of DTA across the
153 environmental index values, calculated using random regression as used in CERIS-JGRA
154 predictions. In all panels, lines connect DTA values of a given genotype across environments;
155 line color indicates genotypic mean. The thick line denotes the common parent B73, and other
156 opaque lines denote other NAM parents.

157

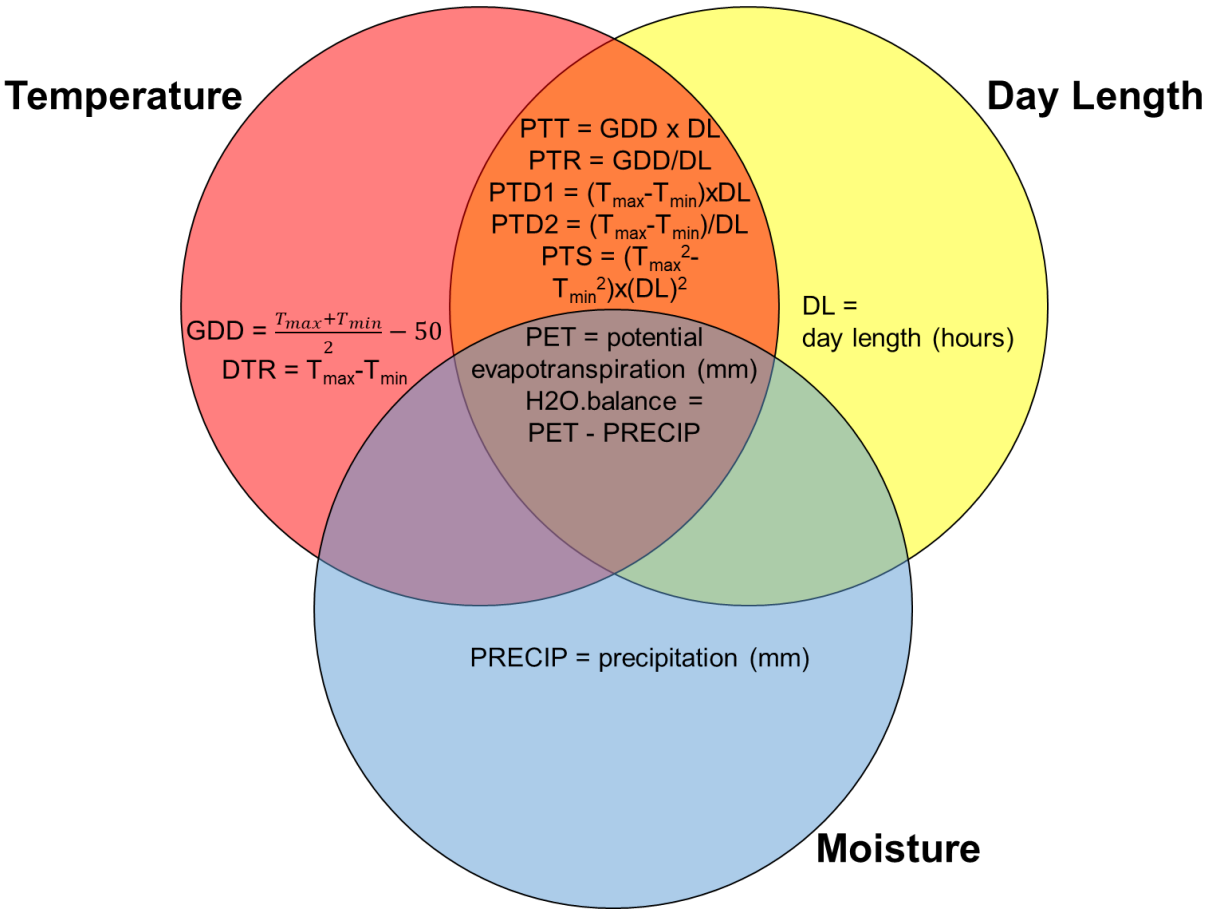

Fig. S3: Environmental variables. The environmental variables searched by CERIS include measures of temperature, day length, moisture, and combinations of these.

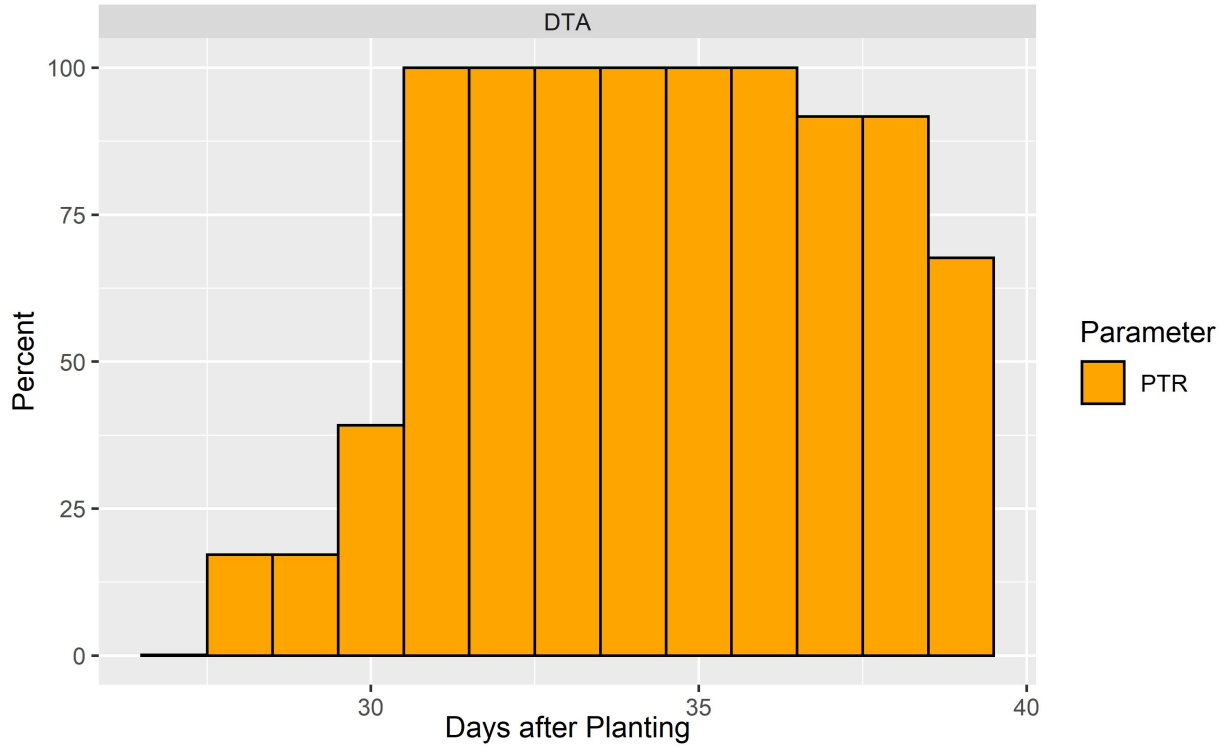

Fig. S4: CERIS-chosen environmental indices are robust to training set. For the example trait DTA, CERIS was conducted on more than 700 different training sets (see Methods). This histogram shows how often a given day after planting was included in the CERIS-chosen environmental index; color indicates the chosen parameter. 100% of training sets yielded environmental indices using the environmental variable PTR and including the time range of 31-36 days after planting.

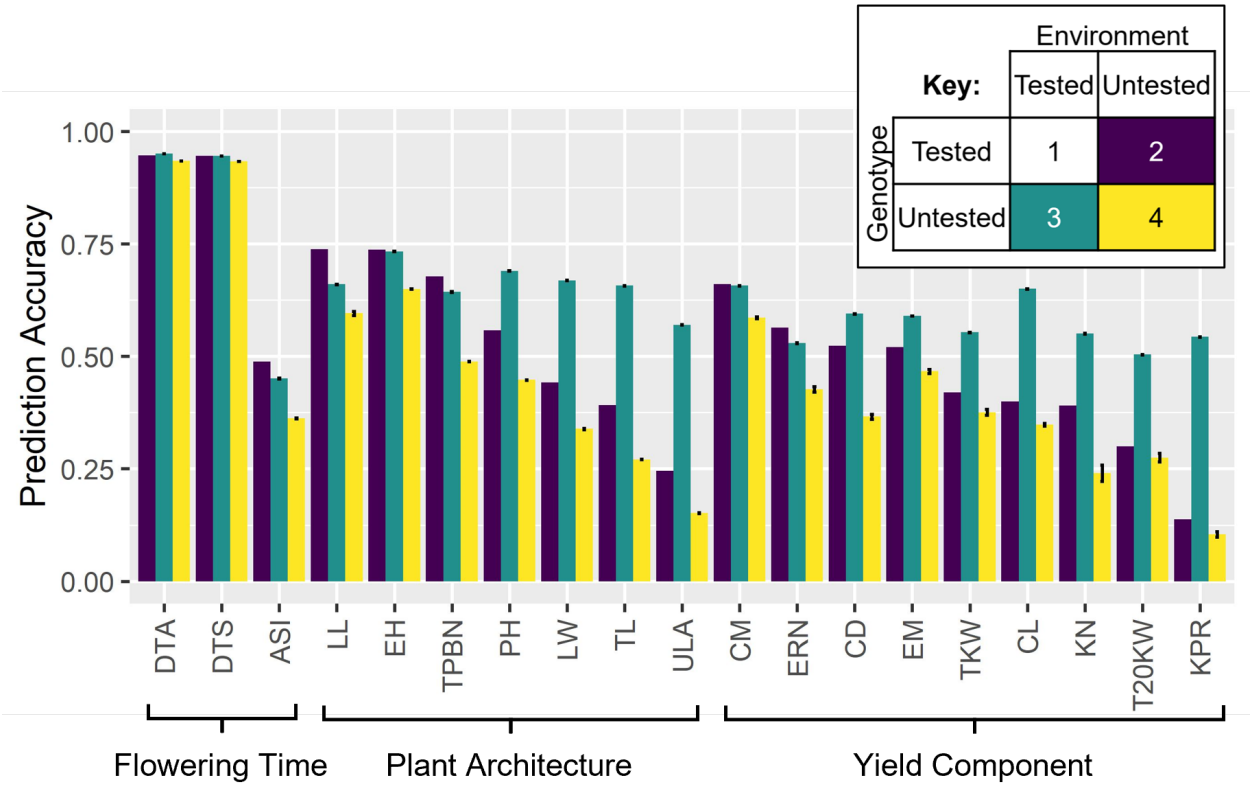

Fig. S5: Prediction accuracy for all traits, overall across all environments. Prediction accuracy for 1 to 2 (purple), 1 to 3 (green), and 1 to 4 (yellow) prediction scenarios for flowering time, plant architecture, and yield component traits. Key (inset) shows naming scheme for prediction scenarios; left and right columns denote tested and untested genotypes, respectively, while the top and bottom rows denote tested and untested genotypes. Error bars show standard error of prediction accuracy from 30 replicates. Traits ordered by prediction accuracy in the 1 to 2 scenario within each trait group.

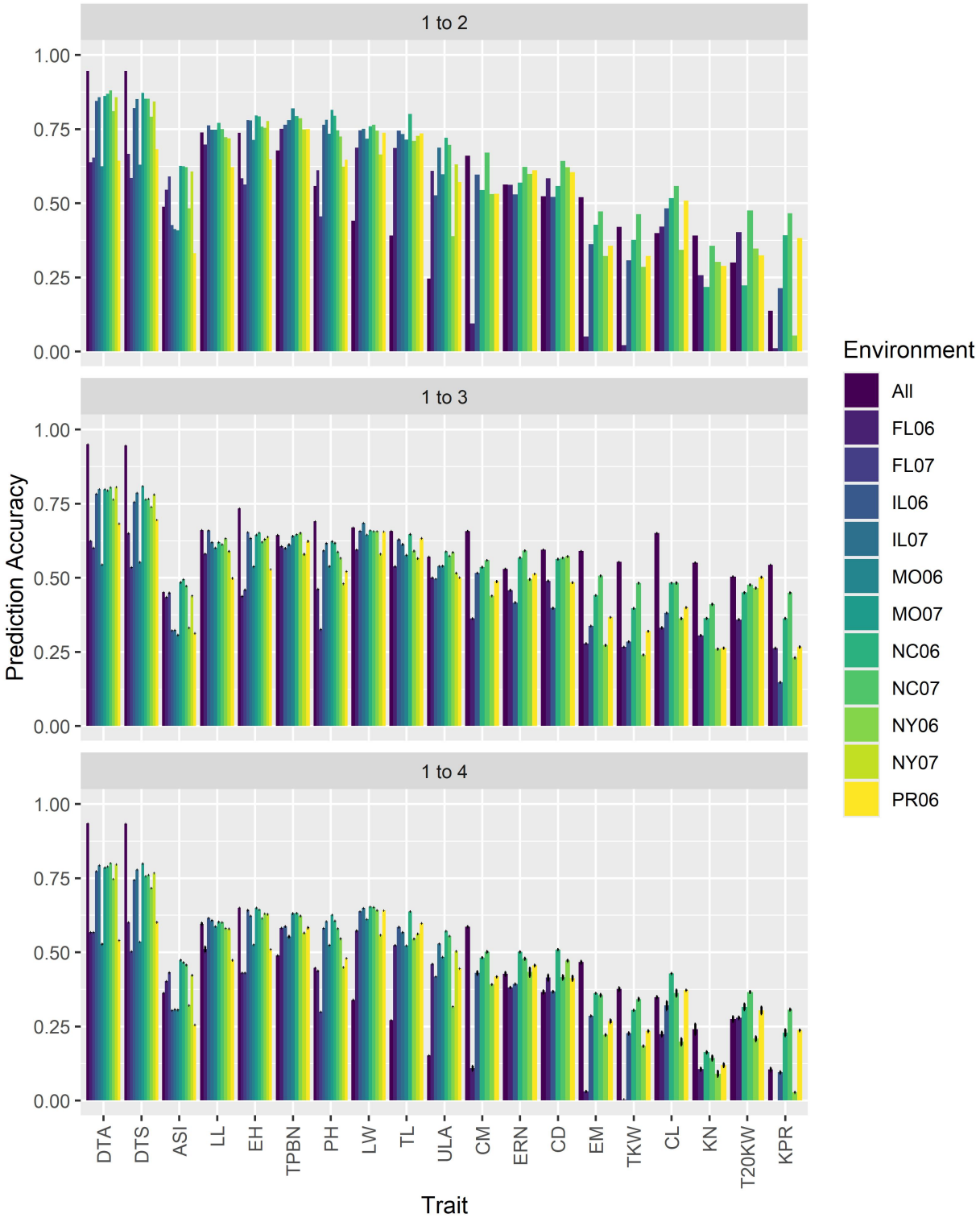
1 to 2
1 to 3
1 to 4
1.00
0.75
0.50
0.25
0.00
Prediction Accuracy
DTA
DTS
ASI
LL
EH
TPBN
PH
LW
TL
ULA
CM
ERN
CD
EM
TKW
CL
KN
T20KW
KPR
Trait
Environment
All
FL06
FL07
IL06
IL07
MO06
MO07
NC06
NC07
NY06
NY07
PR06

Fig. S6: Prediction accuracy for all traits, shown both within and across environments. Prediction accuracy for 1 to 2, 1 to 3, and 1 to 4 prediction scenarios for all traits across environments ("All") as well as within each measured environment. Error bars show standard error of prediction accuracy from 30 replicates. Trait order corresponds to Fig. S5.

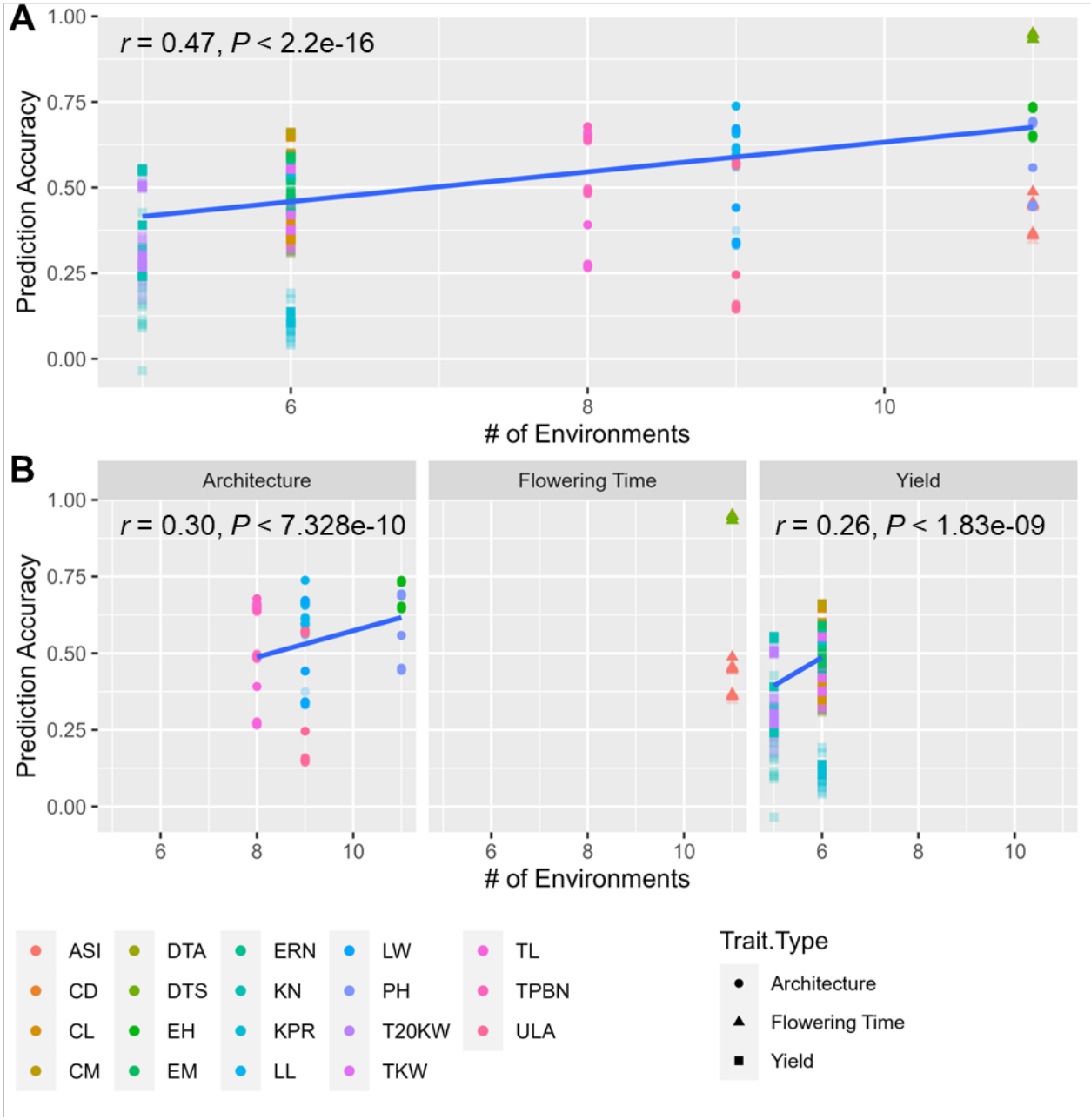

188

189 Fig. S7: Prediction accuracy by number of environments in which each trait was measured. (A)

190 Significant positive correlation found considering all traits together. (B) This correlation decreases when

191 considered separately by trait type.

192

193

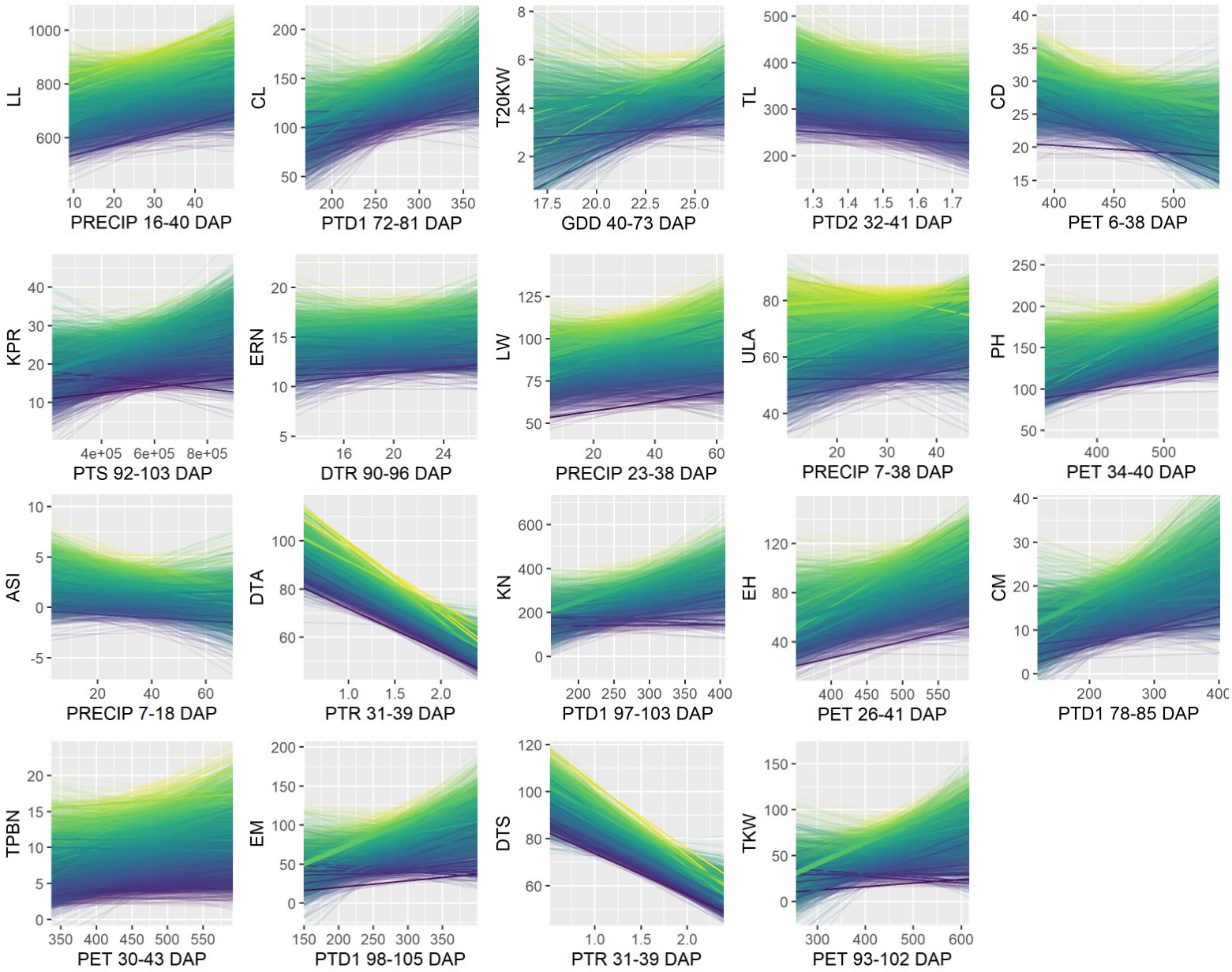
LL
PRECIP 16-40 DAP
CL
PTD1 72-81 DAP
T20KW
GDD 40-73 DAP
TL
PTD2 32-41 DAP
CD
PET 6-38 DAP
KPR
PTS 92-103 DAP
ERN
DTR 90-96 DAP
LW
PRECIP 23-38 DAP
ULA
PRECIP 7-38 DAP
PH
PET 34-40 DAP
ASI
PRECIP 7-18 DAP
DTA
PTR 31-39 DAP
KN
PTD1 97-103 DAP
EH
PET 26-41 DAP
CM
PTD1 78-85 DAP
TPBN
PET 30-43 DAP
EM
PTD1 98-105 DAP
DTS
PTR 31-39 DAP
TKW
PET 93-102 DAP

194

Fig. S8: CERIS reaction norms for all traits. In all panels, the thick line denotes the common parent B73 and opaque lines the other parents; line color indicates the genotypic mean, ranked within a given trait. Slope and intercept estimates from these reaction norms using fixed regression were used as input phenotypes in GWAS. Traits are ordered by the correlation between $-\log_{10}(P)$ values from slope and intercept GWAS to show the continuum of genetic architectures of plasticity.

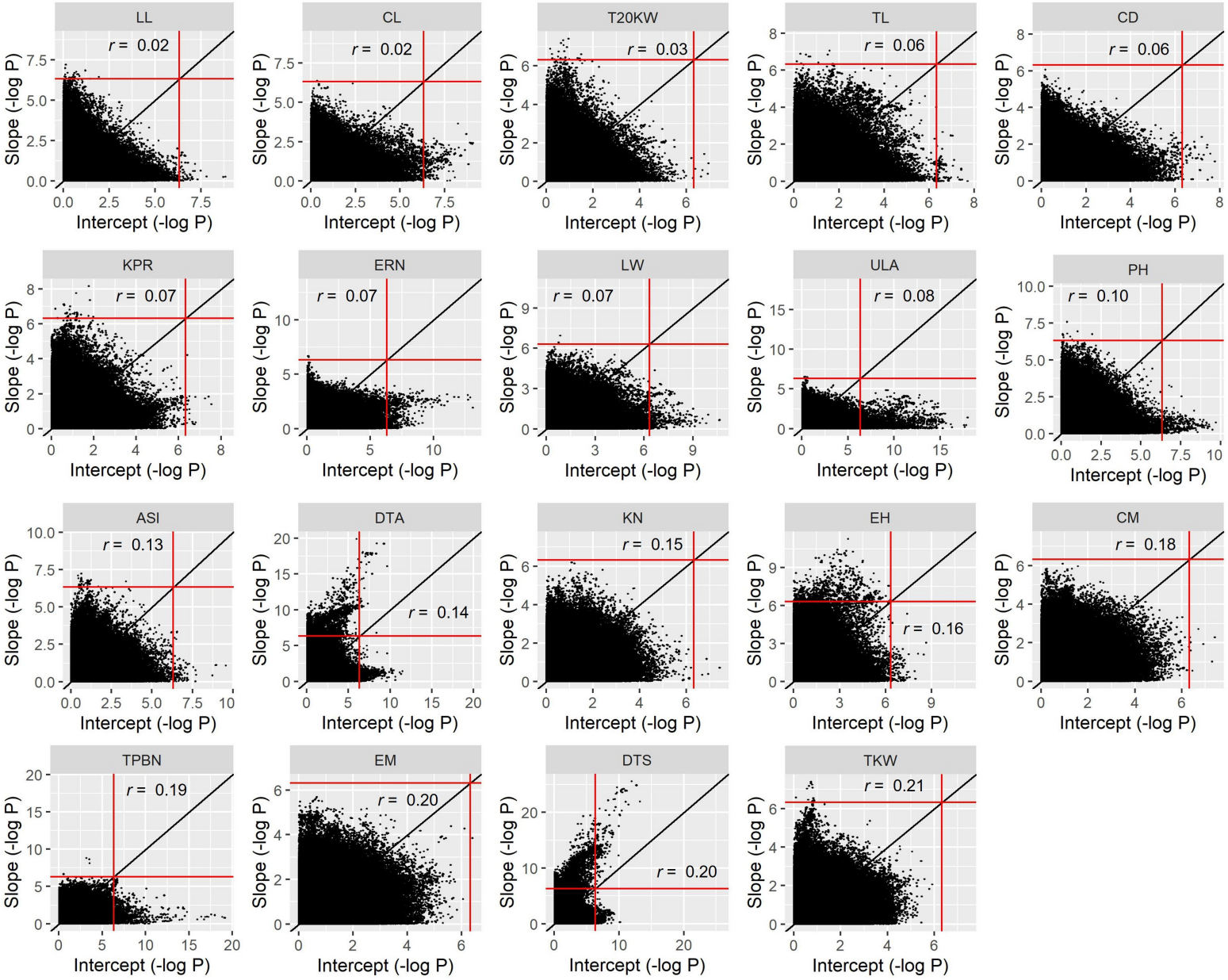
LL
r = 0.02
CL
r = 0.02
T20KW
r = 0.03
TL
r = 0.06
CD
r = 0.06
KPR
r = 0.07
ERN
r = 0.07
LW
r = 0.07
ULA
r = 0.08
PH
r = 0.10
ASI
r = 0.13
DTA
r = 0.14
KN
r = 0.15
EH
r = 0.16
CM
r = 0.18
TPBN
r = 0.19
EM
r = 0.20
DTS
r = 0.20
TKW
r = 0.21
Slope (-log P)
Intercept (-log P)

199

Fig. S9: *P* values of markers from intercept and slope GWAS. For each trait, the $-\log_{10}(P)$ values from slope and intercept GWAS are shown on the y and x axis, respectively. In all cases, these $-\log_{10}(P)$ values were significantly ($P<0.00001$) positively correlated. Red lines show the SimpleM significance threshold, and the black line indicates the line where x = y. Traits ordered by the correlation between $-\log_{10}(P)$ values from slope and intercept GWAS to show the continuum of genetic architectures of plasticity

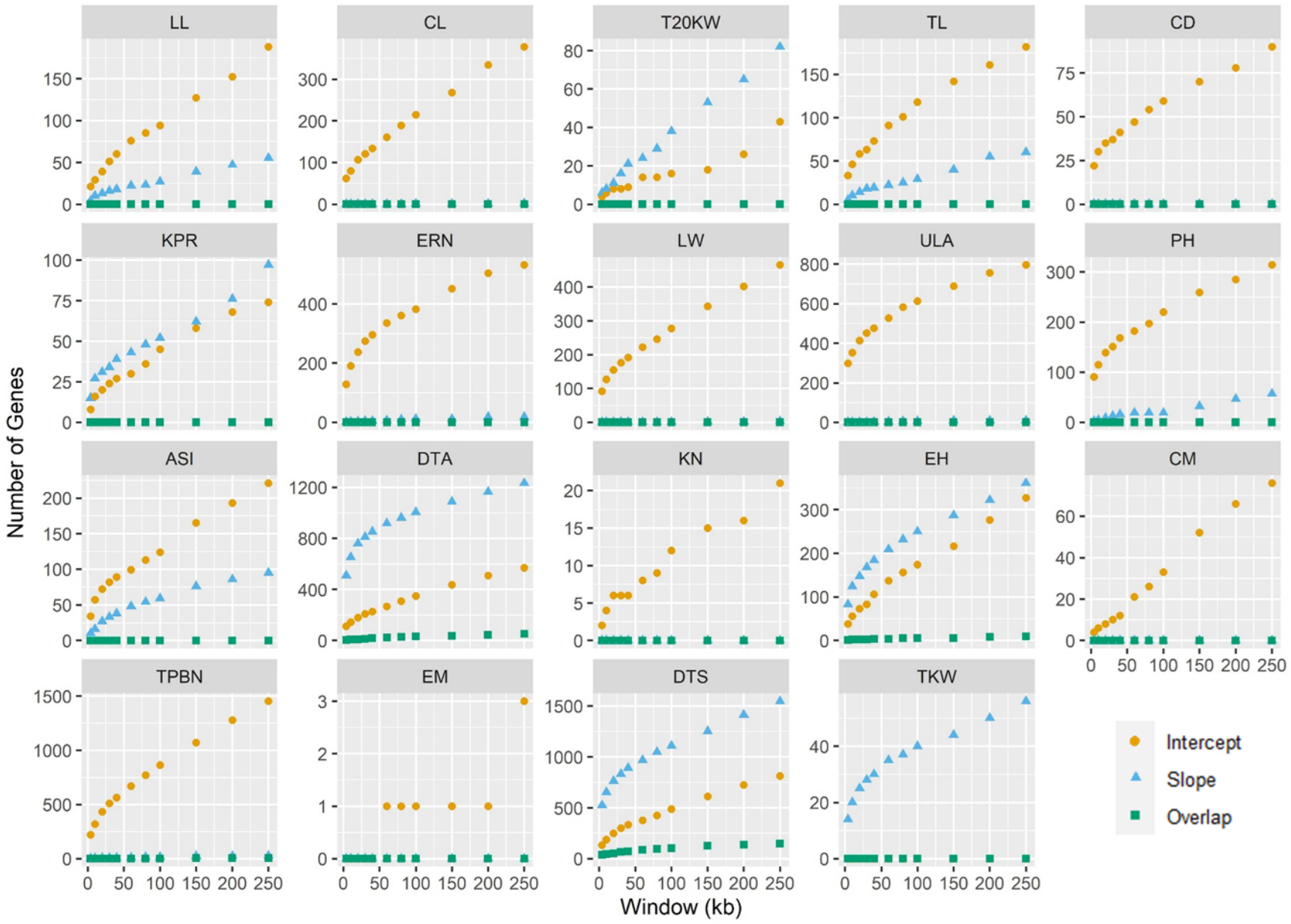
LL
CL
T20KW
TL
CD
KPR
ERN
LW
ULA
PH
ASI
DTA
KN
EH
CM
TPBN
EM
DTS
TKW
Number of Genes
Window (kb)
Intercept
Slope
Overlap

204

Fig. S10: Number of candidate genes by trait for all examined window sizes. Number of genes (y axis) located within a given window (x axis) of significant markers detected in intercept (orange circles) or slope (blue triangles) GWAS as well as those detected in both ("overlap", green squares). Traits ordered by the correlation between $-\log_{10}(P)$ values from slope and intercept GWAS to show the continuum of genetic architectures of plasticity.

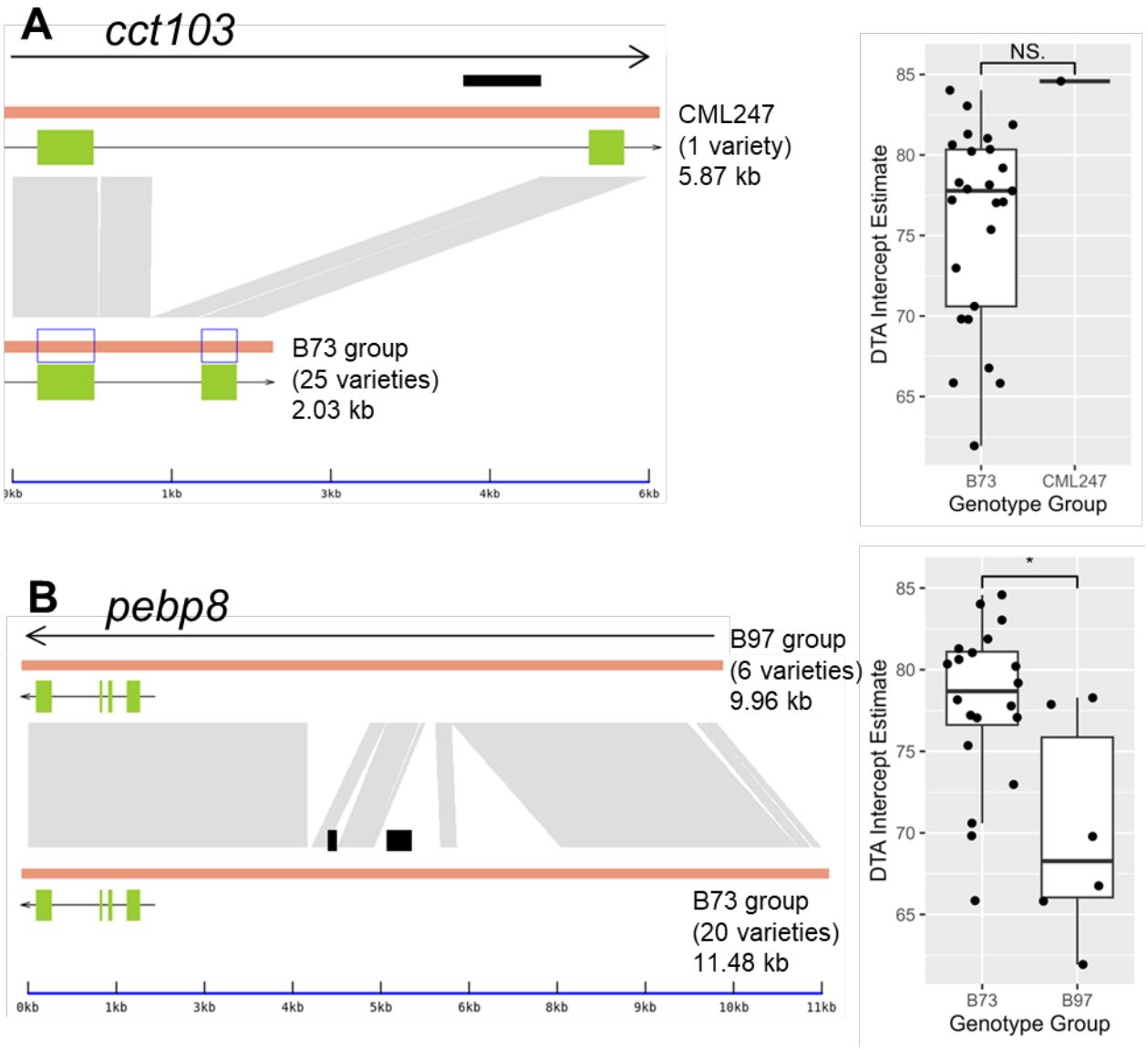
A
cct103
CML247
(1 variety)
5.87 kb
B73 group
(25 varieties)
2.03 kb
1kb
3kb
4kb
6kb
NS.
DTA Intercept Estimate
85
80
75
70
65
B73
CML247
Genotype Group
B
pebp8
B97 group
(6 varieties)
9.96 kb
B73 group
(20 varieties)
11.48 kb
0kb
1kb
3kb
4kb
5kb
6kb
8kb
9kb
10kb
11kb
*
DTA Intercept Estimate
85
80
75
70
65
B73
B97
Genotype Group

Fig. S11: BRIDGEcereal visualization of major haplotypes for DTA intercept candidate genes and associated phenotype estimates among the NAM founders. (A) CML247 has both the highest DTA intercept estimate among the NAM founders and a unique haplotype at *cct103*, distinguished by an insertion in the intron. The CML247 genotype group contains only CML247; the B73 group contains the other 25 founders: B73, B97, CML103, CML228, CML277, CML322, CML333, CML52, CML69, HP301, Il14H, Ki11, Ki3, Ky21, M162W, M37W, Mo18W, MS71, NC350, NC358, Oh43, Oh7B, P39, Tx303, and Tzi8. (B) Polymorphisms upstream of *pebp8* correspond to a significant difference in DTA intercept (B97 group contains B97, Il14H, MS71, Oh7B, P39, and Tx303; B73 group contains B73, CML103, CML228, CML247, CML277, CML322, CML333, CML52, CML69, HP301, Ki11, Ki3, Ky21, M162W, M37W, Mo18W, NC350, NC358, Oh43, and Tzi8).

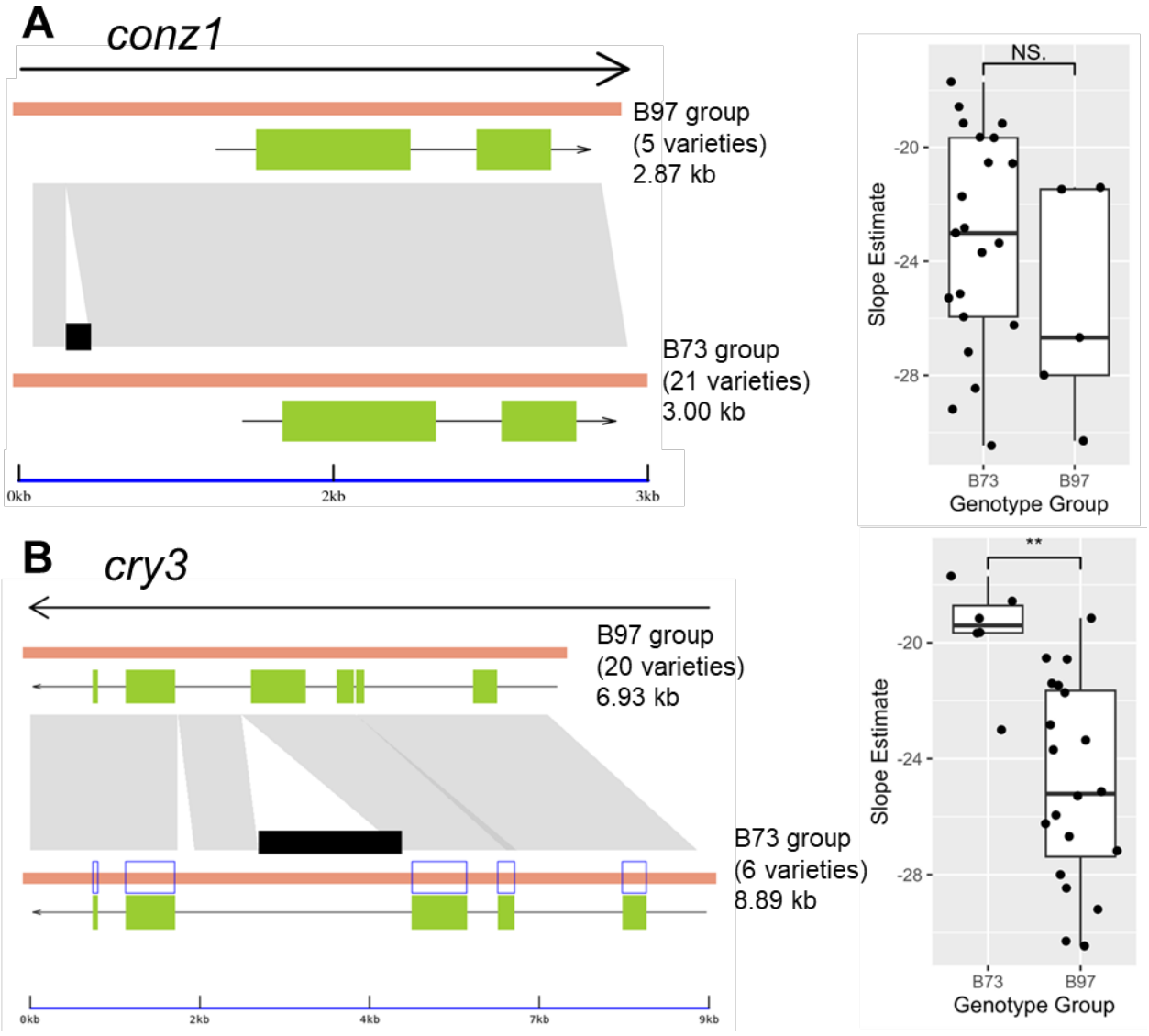

Fig. S12: BRIDGEcereal visualization of major haplotypes for DTA slope candidate genes and associated phenotype estimates among the NAM founders. (A) A small insertion is present upstream of *conz1* but is not significantly associated with a change in slope (B97 group contains B97, CML322, CML333, Ki11, and MS71; B73 group contains B73, CML103, CML228, CML247, CML277, CML52, CML69, HP301, Il14H, Ki3, Ky21, M162W, M37W, Mo18W, NC350, NC358, Oh43, Oh7B, P39, Tx303, and Tzi8). (B) An insertion within the second exon of *cry3* is significantly associated with a steeper DTA slope (B73 group contains B73, HP301,

232 Il14H, Oh7B, Oh43, and P39; B97 group contains B97, CML103, CML228, CML247, CML277,
233 CML322, CML333, CML52, CML69, Ki11, Ki3, Ky21, M162W, M37W, Mo18W, MS71,
234 NC350, NC358, Tx303, and Tzi8)
235
236

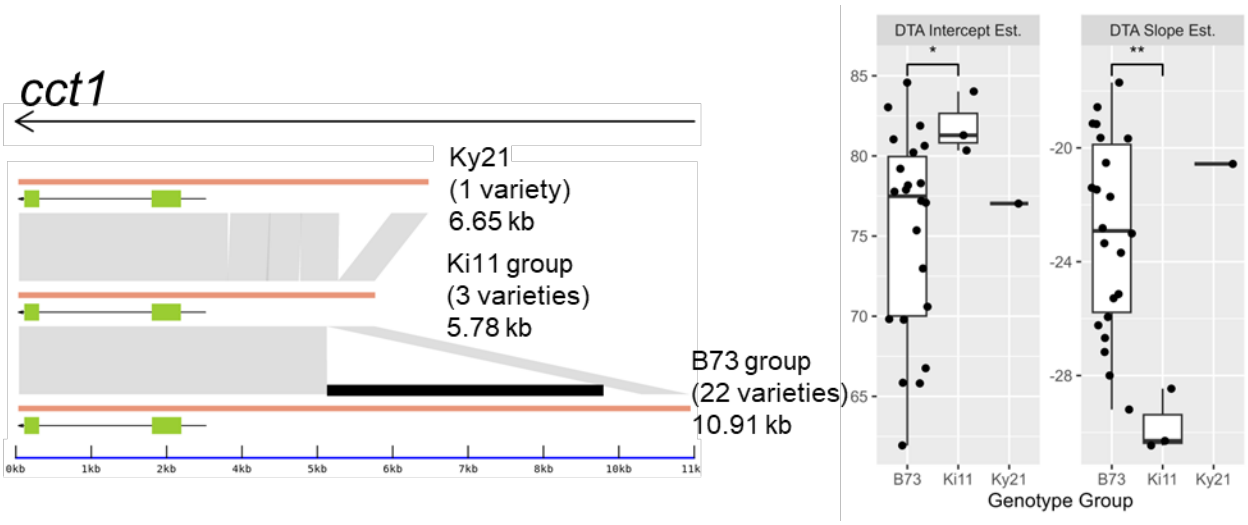

Fig. S13: BRIDGEcereal visualization of major haplotypes for *cct1*, the selected candidate gene identified for both DTA slope and intercept, and associated phenotype estimates among the NAM founders. The CACTA-like insertion identified upstream of *cct1* in CML228, CML277, and Ki11 (Ki11 group) is a known allele that reduces *cct1* expression and thereby reduces flowering time (DTA intercept). Here, this allele was also significantly associated with a steeper DTA slope. In addition, a potential weak allele was identified in Ky21 (single member of Ky21 group). B73 group contains B73, B97, CML103, CML247, CML322, CML333, CML52, CML69, HP301, Il14H, Ki3, M162W, M37W, Mo18W, MS71, NC350, NC358, Oh43, Oh7B, P39, Tx303, and Tzi8.

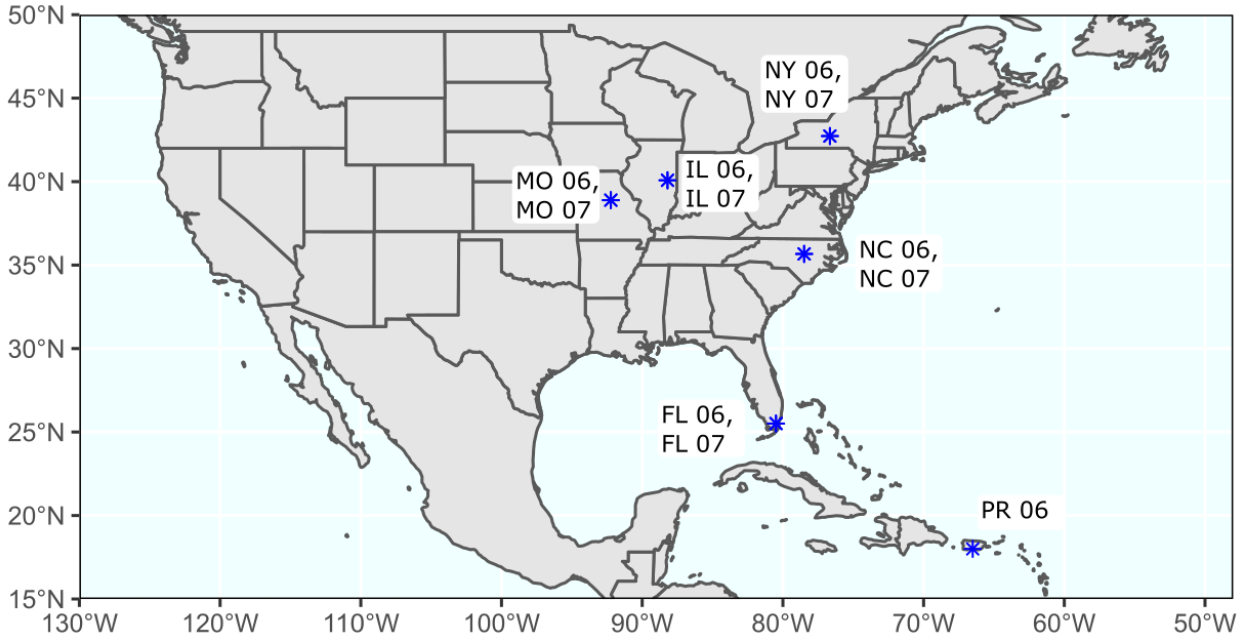

Fig. S14: Study environments map. Data was collected at 6 locations (blue asterisks) over two years. Environment names consist of the two-letter state abbreviation and the last two digits of the year (e.g., MO06 is Missouri 2006).

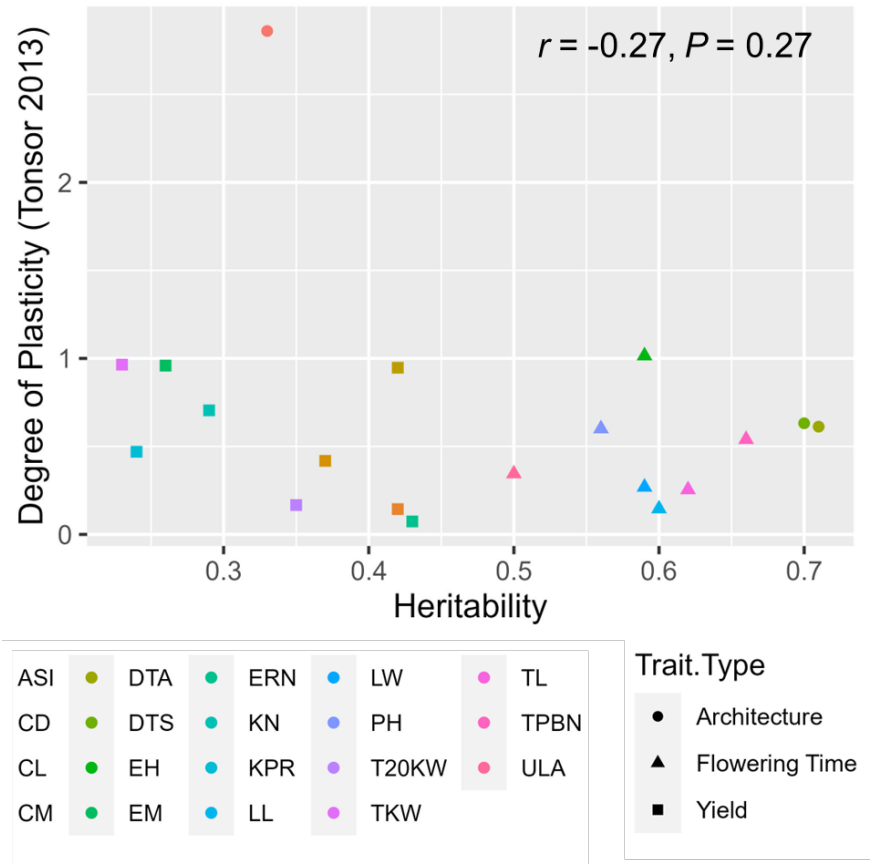

253

254 Fig. S15: Heritability (h_p^2) and degree of plasticity (calculated per Tonsor et al. 2013) are not

255 significantly correlated in the maize NAM.

256

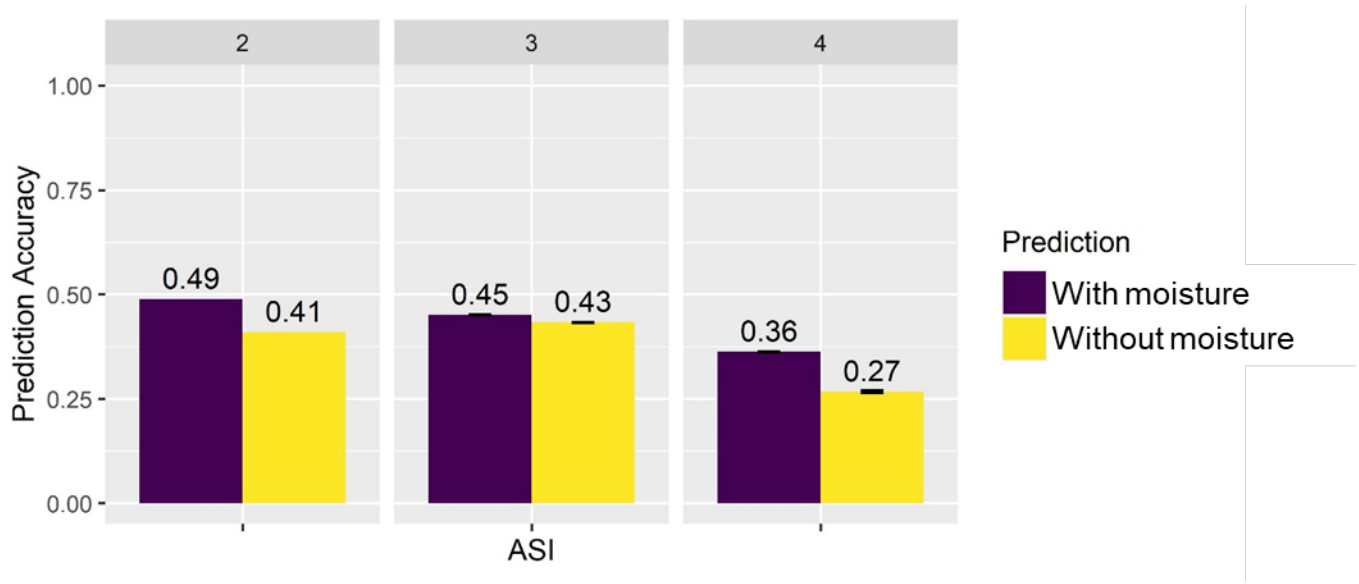

257

258 Fig. S16: Prediction accuracy for Anthesis-Silking Interval (ASI) with and without moisture
259 variables. When including variables involving moisture (precip, PET, and water balance) in the
260 CERIS search space (purple), prediction accuracy improved significantly for ASI. Error bars
261 show standard error of prediction accuracy based on 30 replicates with and 5 replicates without
262 moisture variables.

263

Supplemental Tables

Table S1: List of traits. Abbreviations, full names, types, number of environments measured in (# Envs), measurement time, and search windows for all nineteen traits examined in this study. Measurement time indicates the time during the growing season at which this trait was measured, and search window indicates the range of days after planting that were searched by CERIS for this trait to ensure that no prediction was based on a window after the trait had been measured.

Trait Abbreviation	Trait Name	Trait Type	# Envs	Measurement Time	Search Windows
ASI	Anthesis-Silking Interval	Flowering Time	11	Flowering Time	1 – 46
CD	Cob Diameter	Yield	6	Harvest	1 – 106
CL	Cob Length	Yield	6	Harvest	1 – 106
CM	Cob Mass	Yield	6	Harvest	1 – 106
DTA	Days to Anthesis	Flowering Time	11	Flowering Time	1 – 46
DTS	Days to Silking	Flowering Time	11	Flowering Time	1 – 46
EH	Ear Height	Plant Architecture	11	Flowering Time	1 – 46
EM	Ear Mass	Yield	6	Harvest	1 – 106
ERN	Ear Row Number	Yield	6	Harvest	1 – 106
KN	Kernel Number	Yield	5	Harvest	1 – 106
KPR	Kernels per Row	Yield	6	Harvest	1 – 106
LL	Leaf Length	Plant Architecture	9	Flowering Time	1 – 46
LW	Leaf Width	Plant Architecture	9	Flowering Time	1 – 46
PH	Plant Height	Plant Architecture	11	Flowering Time	1 – 46
T20KW	Weight of 20 Kernels	Yield	5	Harvest	1 – 106
TKW	Total Kernel Weight	Yield	6	Harvest	1 – 106
TL	Tassel Length	Plant Architecture	8	Flowering Time	1 – 46
TPBN	Tassel Branch Number	Plant Architecture	8	Flowering Time	1 – 46
ULA	Upper Leaf Angle	Plant Architecture	9	Flowering Time	1 – 46

Table S2: CERIS-chosen environmental indices. Environmental indices identified by CERIS for each trait using all available data. For each trait, the environmental index consists of a window and environmental variable (env.variable). The window's start and end are presented as days after planting (DAP). The correlation between the chosen environmental index (EI) and the environmental mean (EM) is shown as $r_{EI,EM}$.

Trait Abbreviation	Start (DAP)	End (DAP)	Env. Variable	$r_{EI,EM}$
ASI	7	18	PRECIP	-0.8773
CD	6	38	PET	-0.9981
CL	72	81	PTD1	0.9930
CM	78	85	PTD1	0.9998
DTA	31	39	PTR	-0.9964
DTS	31	39	PTR	-0.9964
EH	26	41	PET	0.9201
EM	98	105	PTD1	0.9988
ERN	90	96	DTR	0.9822
KN	97	103	PTD1	0.9987
KPR	92	103	PTS	0.9879
LL	16	40	PRECIP	0.9645
LW	23	38	PRECIP	0.8233
PH	34	40	PET	0.8889
T20KW	40	73	GDD	0.9989
TKW	93	102	PET	0.9991
TL	32	41	PTD2	-0.8851
TPBN	30	43	PET	0.8772
ULA	7	38	PRECIP	0.7363

Table S3: Significant markers. Contains markers detected as significant by GWAS for each trait (slope and intercept) using a SimpleM threshold ($\alpha = 0.05$). The first three columns contain chromosome, base pair location, and name for each significant marker. Subsequent columns are traits. A blank (NA) cell indicates that the marker was not detected for that trait, while numbers indicate *P* values for significant markers.

Note: Table S3 is attached as "Supplemental_Table_S3.csv"

Table S4: Candidate genes. Contains candidate genes detected by GWAS for each trait (slope and intercept) using a 20kb window around each significant marker. The first column contains all gene names from Zm-B73-REFERENCE-NAM-5.0 which were significant for at least one trait and the first row contains trait names. A "1" in a cell means that that gene was detected as a candidate gene for that trait, and a "0" means that it was not.

Note: Table S4 is attached as "Supplemental_Table_S4.csv"

Table S5: Enriched GO terms. Cells contain g:SCS multiple testing correction adjusted *p* values; cells with significant values are shaded gray and marked with an asterisk. Candidate genes within 20kb of significant markers from slope and intercept GWAS were analyzed for GO term enrichment. This analysis was conducted for the combined gene lists from all traits as well as within trait groups (Flowering Time, Yield, and Plant Architecture).

GO Term Name	GO Term ID	All Traits		Flowering Time		Plant Architecture		Yield	
		Intercept	Slope	Intercept	Slope	Intercept	Slope	Intercept	Slope
Ubiquinol:oxygen oxidoreductase activity	GO:0102721	*0.00004	1.00000	1.00000	1.00000	*0.00016	1.00000	1.00000	1.00000
Alternative oxidase activity	GO:0009916	*0.00004	1.00000	1.00000	1.00000	*0.00016	1.00000	1.00000	1.00000
Oxidoreductase activity, acting on diphenols and related substances as donors, oxygen as acceptor	GO:0016682	*0.00203	1.00000	1.00000	1.00000	*0.00069	1.00000	1.00000	1.00000
Oxidoreductase activity, acting on diphenols and related substances as donors	GO:0016679	*0.02732	1.00000	1.00000	1.00000	*0.00665	1.00000	1.00000	1.00000
RNA-directed 5'-3' RNA polymerase activity	GO:0003968	1.00000	0.09460	1.00000	*0.03676	1.00000	1.00000	1.00000	1.00000
ATPase-coupled intramembrane lipid transporter activity	GO:0140326	1.00000	*0.04653	1.00000	0.23530	1.00000	1.00000	1.00000	1.00000
Alternative respiration	GO:0010230	*0.00089	1.00000	1.00000	1.00000	*0.00214	1.00000	1.00000	1.00000
Detoxification	GO:0098754	1.00000	0.47270	1.00000	*0.03830	1.00000	1.00000	1.00000	1.00000
Response to toxic substance	GO:0009636	1.00000	0.56234	1.00000	*0.04288	1.00000	1.00000	1.00000	1.00000
Cellular oxidant detoxification	GO:0098869	1.00000	0.45173	1.00000	*0.04711	1.00000	1.00000	1.00000	1.00000
Plant hormone signal transduction	KEGG:04075	*0.02339	1.00000	1.00000	1.00000	*0.02313	1.00000	1.00000	1.00000
Biosynthesis of secondary metabolites	KEGG:01110	1.00000	*0.02882	1.00000	0.23211	1.00000	1.00000	1.00000	1.00000

299

Table S6: Within-environment heritability. Heritability on an individual plot basis (h_p^2) for each trait in each environment. Blank cells indicate environments in which the specified trait was not measured.

	IL06	FL06	MO06	NC06	NY06	PR06	IL07	FL07	MO07	NC07	NY07
ASI	0.24	0.44	0.20	0.55	0.42	0.43	0.25	0.63	0.67	0.59	0.34
CD	0.39	0.53		0.64	0.60	0.59				0.77	
CL	0.45	0.40		0.62	0.56	0.53				0.73	
CM	0.66	0.46		0.64	0.69	0.58				0.77	
DTA	0.86	0.79	0.81	0.86	0.85	0.71	0.87	0.88	0.93	0.92	0.70
DTS	0.87	0.74	0.83	0.85	0.69	0.77	0.84	0.83	0.92	0.91	0.66
EH	0.76	0.68	0.60	0.79	0.66	0.67	0.75	0.73	0.77	0.77	0.77
EM	0.55	0.42		0.58	0.61	0.55				0.81	
ERN	0.64	0.60		0.69	0.57	0.58				0.77	
KN		0.54		0.58	0.69	0.59				0.84	
KPR	0.22	0.34		0.53	0.63	0.46				0.72	
LL	0.80	0.71	0.65	0.71	0.67	0.65	0.73			0.65	0.59
LW	0.65	0.66	0.59	0.68	0.54	0.69	0.71			0.75	0.62
PH	0.83	0.71	0.65	0.83	0.58	0.70	0.76	0.69	0.83	0.77	0.68
T20KW		0.39		0.61	0.61	0.65				0.76	
TKW	0.41	0.42		0.56	0.63	0.54				0.81	
TL	0.77	0.72	0.66	0.78	0.70	0.71	0.76				0.73
TPBN	0.73	0.62	0.71	0.72	0.63	0.75	0.70				0.67
ULA	0.60	0.62	0.39	0.68	0.62	0.45	0.63			0.78	0.58